Automated tool-path generation for rapid manufacturing and numerical simulation of additive manufacturing LMD geometries

M. Biegler*[1], J. Wang[1], B. Graf[1], M. Rethmeier[1,2,3]
[1] *Fraunhofer Institute of Production Systems and Design Technology (IPK), Berlin, Germany*
[2] *Federal Institute of Materials Research and Testing (BAM)*
[3] *Institute of Machine Tools and Factory Management, Technical University Berlin*

*Corresponding Author: e-mail max.biegler@ipk.fraunhofer.de

Summary
In additive manufacturing (AM) Laser Metal Deposition (LMD), parts are built by welding layers of powder feedstock onto a substrate. Applications for steel powders include forging tools and structural components for various industries. For large parts, the choice of tool-paths influences the build-rate, the part performance and the distortions in a highly geometry-dependent manner. With weld-path lengths in the range of hundreds of meters, a reliable, automated tool path generation is essential for the usability of LMD processes.
In this contribution, automated tool-path generation approaches are shown and their results are discussed for arbitrary geometries. The investigated path strategies are the classical approaches: “Zig-zag-” and “contour-parallel-strategies”. After generation, the tool-paths are automatically formatted into g-code for experimental build-up and ASCII for a numerical simulation model. Finally, the tool paths are discussed in regards to volume-fill, microstructure and porosity for the experimental samples.
This work presents a part of the IGF project 18737N “Welding distortion simulation” (FOSTA P1140)

Key Words
Additive Manufacturing, Directed Energy Deposition, Path planning, DED, Mechanical properties, Porosity

Introduction
As additive manufacturing Laser Metal Deposition (LMD) is a relatively new process, little formalized guides exist for build-up of individual parts. Apart from optimizing process parameters such as laser power, forward speed and feedstock flow [1], the infill pattern is playing a significant role for part quality [2]. Foroozmehr et al. [3] showed that different infill strategies ranging from zig-zag patterns to spirals lead to different temperature flows and resulting residual stresses. Although the automated tool-path generation is generally documented in the literature for CNC milling applications, differences present themselves for additive manufacturing, because the part is constructed rather than reduced during the process and constant material deposition as well as heat management are crucial to the process.
Figure 1 shows a standard workflow for LMD pre-processing from the CAD model to the path planning on the LMD machine. The aim of this publication is to

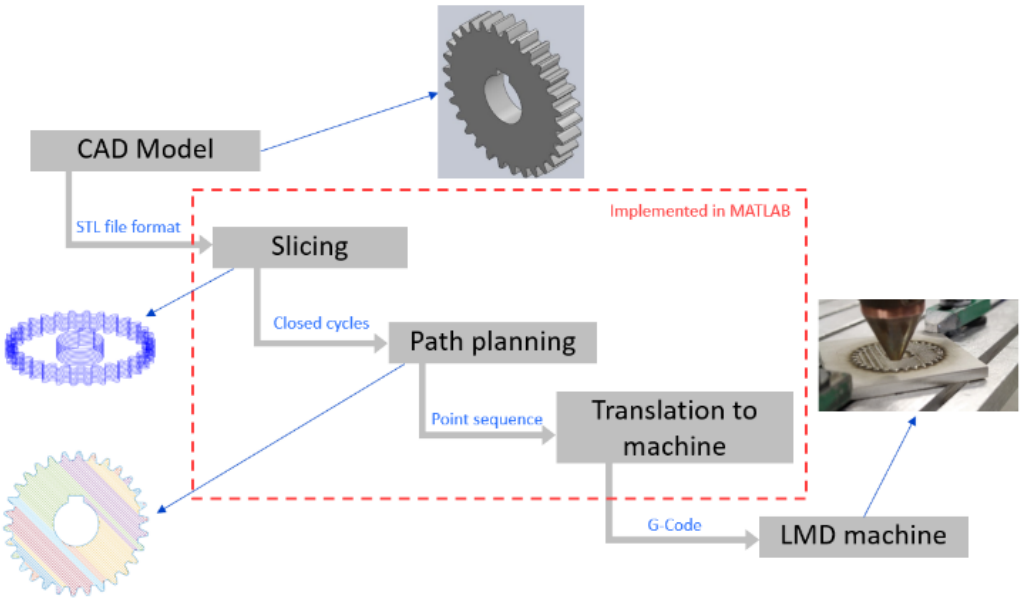

Figure 1: Standard workflow in part setup for the LMD process. Slicing, path planning and translation to the machine has been implemented for this work

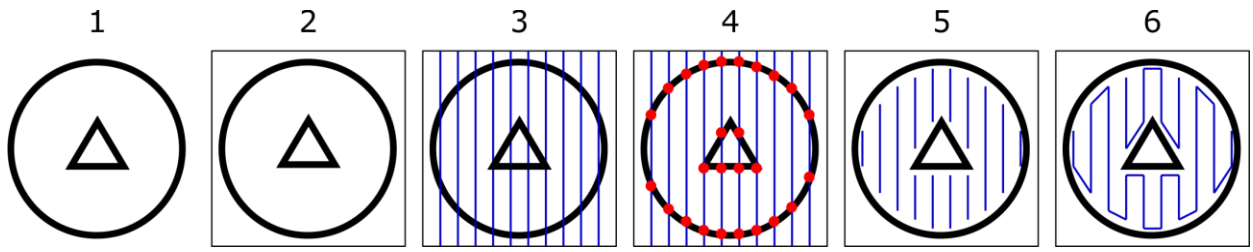

Figure 2:: The six steps necessary to generate a tool path in a sliced 2D geometry.

demonstrate the implementation of two automated path-planning strategies for LMD, i.e. zig-zag and contour-parallel approaches. Subsequently, a geometry is built with both strategies and the usability is discussed according to the cross-section and the final shape accuracy.

Zig-zag strategy

The implementation of the zig-zag path planning strategy is visualized in Figure 2 and follows these 6 steps:

1. 2D area generation by slicing 3D geometry
2. Identification of the smallest bounding box enclosing the 2D area
3. Splitting the bounding box with equidistant lines
4. Finding intersection points between all the lines with the boundary of the 2D area, typically there are multiples of two points per line
5. Trimming the line segments from the points and construction of line segments from these points with offset from the boundary
6. Connection of ending (or starting) points of each neighbor to form a continuous path

It is common that more than one continuous path is created during step 6. In order to prevent the generation of multiple sub-paths for one layer, the inclination angle of the equidistant lines in step 3 have to be chosen appropriately. Single continuous infill paths can be created, if the surrounding polygon chain is monotone with respect to a straight line, i.e. the straight lines from point 3 only intersect the sliced geometry twice. If the monotone condition is not met, sub-paths are generated, where the manufacturing head has to switch off the laser and move to the next path's beginning.

Contour-parallel strategy

The contour-parallel pattern displaces outer contours of the sliced geometry inward and inner contours outward in turn.

1. The 2D boundary contour obtained during slicing is used as an input for this algorithm. Each cycle is either assigned the property *internal cycle* or *external cycle* according to their location. An *internal cycle* is always expanded during offset, whereas an *external cycle* is shrunk.
2. The path generation process is initiated. This loop will run until no cycles are created during the offset. After termination, the path generation is finished and a matrix contains the trajectories of each tool-path generated in this process.
3. If there are intersections between contours, there are two possible scenarios:

(a) Intersection between two *internal cycles*: The union of both intersecting cycles is created and the resulting cycle is assigned the property *internal cycle* and then merged with the current set of cycles. An example of two intersecting *internal cycles* creating one new *internal cycle* is illustrated in case a) of

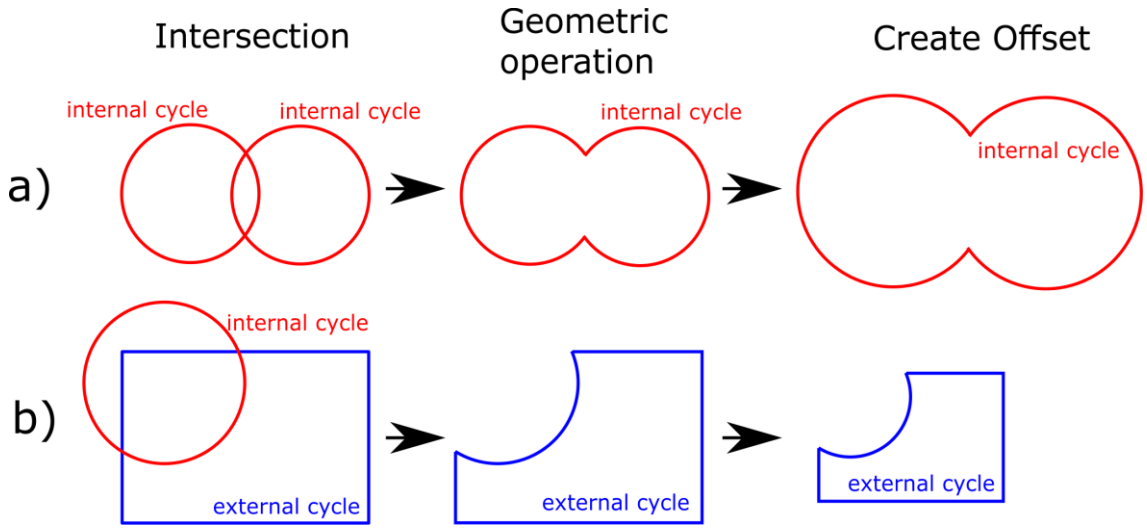

Figure 3: The two special cases encountered while generating contour parallel paths: a

Figure 3. The resulting cycle is inflated during the offset.

(b) Intersection between an *internal* and *external cycle*: A set difference is created, where the *internal cycle* is subtracted from the *external* one. The resulting cycle is assigned the property *external cycle* and then merged with the current set of cycles. Case b) in Figure 3 depicts this scenario. The resulting *external cycle* shrinks during the offset.

Experimental procedure

The experiments were conducted onto an EN 1.4404 (AISI 316L) hot rolled and squared steel substrate with 100 mm side length and 8 mm thickness. The samples were cleaned before the welding process and both sides were rigidly clamped onto the table. The TRUMPF TruLaser Cell 7020 equipped with a 2 kW disc laser and a TRUMPF coaxial powder nozzle to direct the powder flow and argon shielding gas was deployed as cladding system. The geometry to be filled was chosen to be a turbine-blade cross section. This geometry was used in prior investigations by the authors [4] that could be continued here. For the direction-parallel strategy the infill of each manufactured layer alternated between an inclination angle of 45° and 135° (Figure 4 left side). The chosen inclination angles led to monotone polygons and therefore continuous paths were created for each layer. The layers of the contour-parallel method alternated between a 1 mm and a 0.95 mm step over distance among its infill cycles, resulting into seven and eight infill cycles each (Figure 4 right side respectively). The alternating distances created an overlap and avoided the gaps between each cycle in a layer. The infill paths in uneven layers are fabricated from outer to inner cycle, whereas the paths in even layers are ordered from inner to outer cycle.

During the preliminary experiments it was concluded that a bead width of 1.3 mm was suitable for this experiment. The following process parameters could achieve that width:

- Laser power: 600 W
- Beam spot diameter: 0.6 mm
- Forward speed: 600 mm/min
- Powder flow rate: 3.5 g/min

In each layer the processing head first moved along the contour and then filled out the area. This was done four times consecutively with the two alternating infill patterns for each strategy. Additionally, the starting point on the contour for each layer was set to different positions to avoid the deposited material to pile up. Due to the increasing slope towards the boundary contour after each manufactured layer, an extra layer only consisting of the boundary contour was welded on top. The whole procedure is repeated until the total height of the blade exceeded 10 mm. The layer offset of the direction-parallel method was set to 0.7 mm. Similarly, the layer offset for the contour-parallel

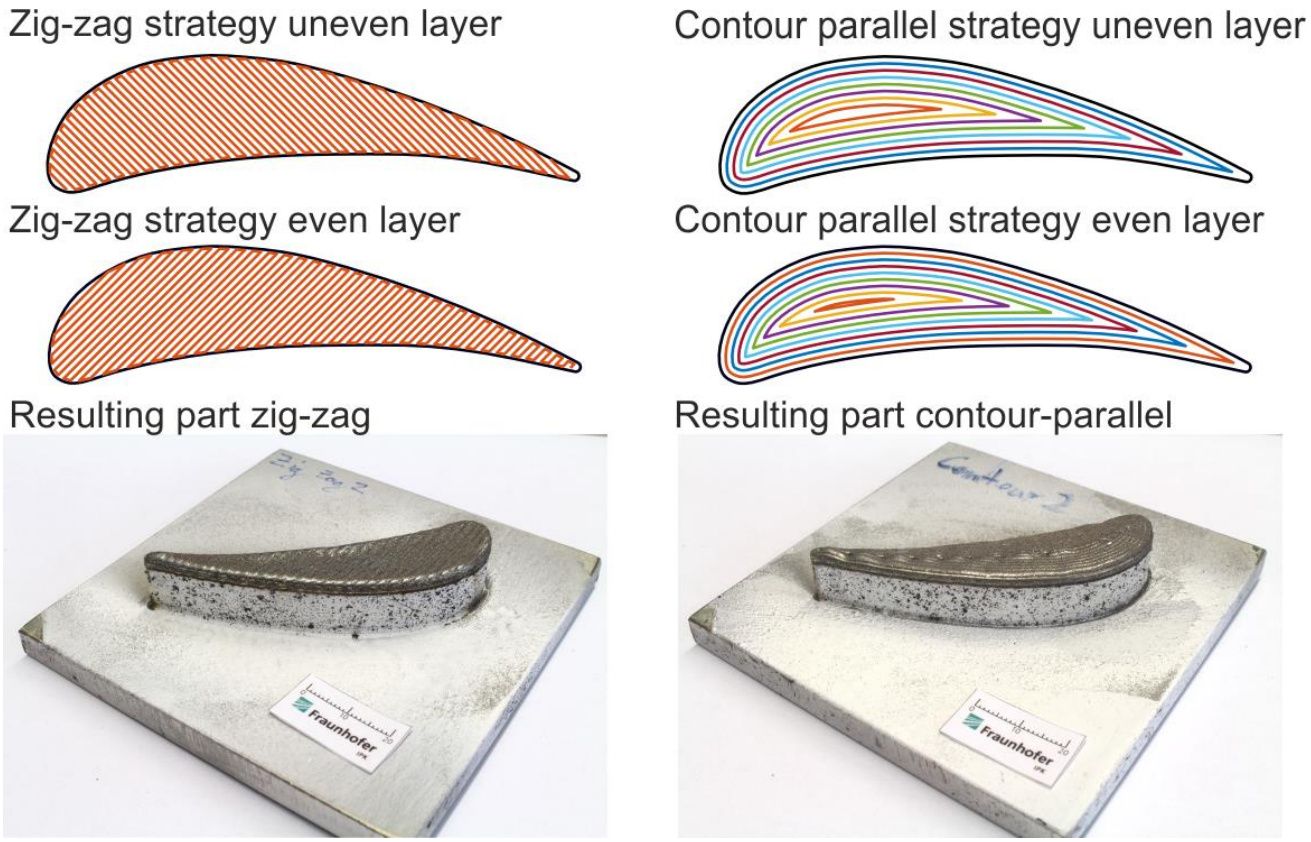

Figure 4: Fill strategies and final parts for both strategies.

approach was set to 0.5 mm. Therefore, six routines consisting of four consecutively fabricated layers and one extra layer only consisting of the boundary contour were needed. The lower achieved height was probably caused by lower concentrated heat in the contour-parallel case that led to a lower powder efficiency. There was a 30 s pause between each layer for cooling [5]. For all the experiments the 316L powder feedstock (Metco 41C, grain size 45-90 µm [6] was used as welding material.

Results

To judge the success of the different path planning strategies, a cross section for one sample of each experiment was made. The cross sections and close-ups for the direction-parallel and contour-parallel sample are shown in Figure 5.

The top surface of the zig-zag sample is slightly bending downwards, whereas material is piling up in the center of the contour-parallel sample. 2-3 additional layers only consisting of the outer contours are welded on top of the sample prior to continuing the process to keep the edges from sagging down. These layers can be detected on both samples by the slight overhang on the left and right of the side surface.

Pores can be found in both samples. They can be caused by absorption of the welding gas in the molten weld pool due to poor gas shielding or by poor quality of the metal powder. In the contour-parallel sample, three large pores can be detected in the center of the

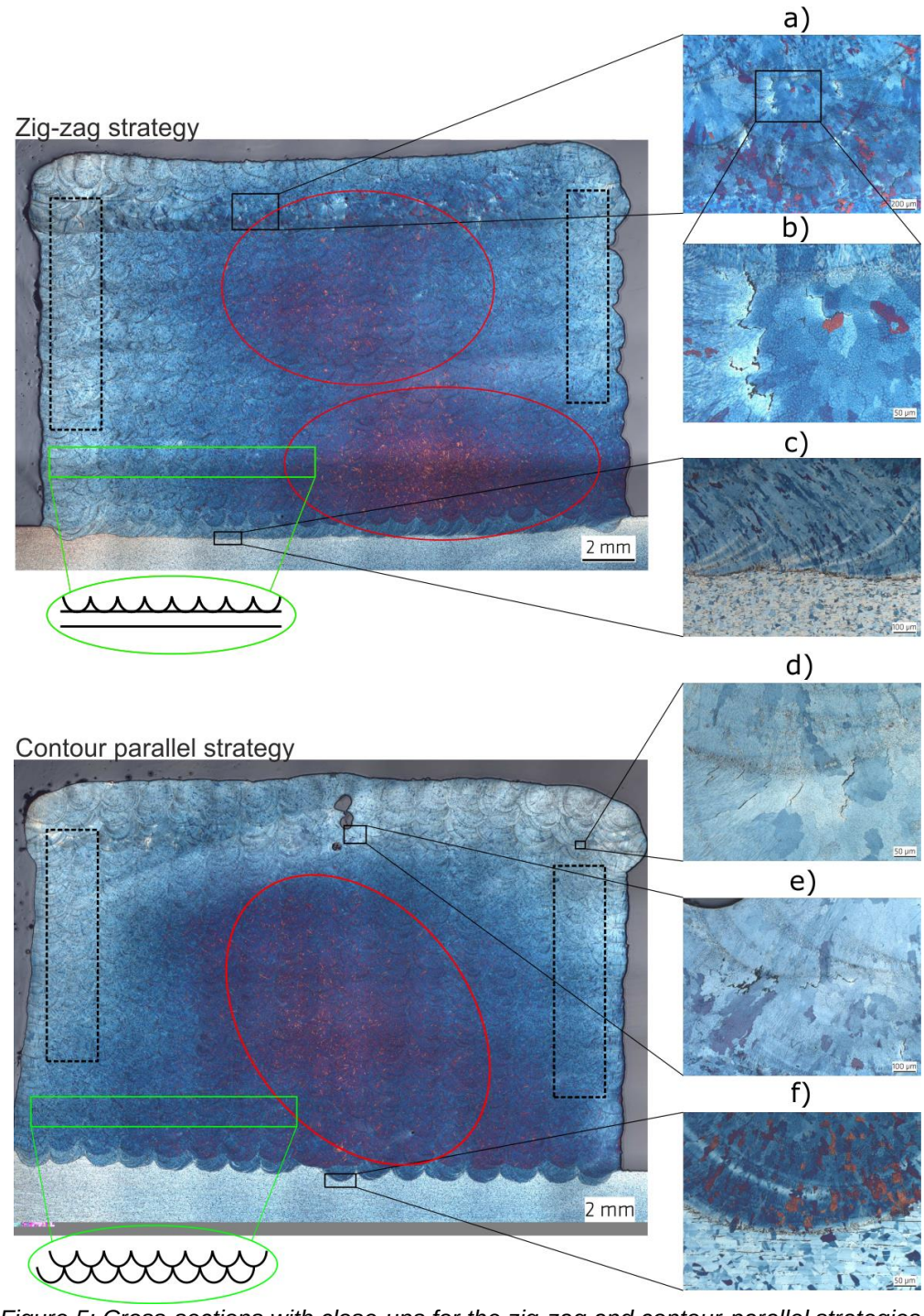

Figure 5: Cross-sections with close-ups for the zig-zag and contour-parallel strategies..

top layers. These pores result from the path planning rather than being the result of poor gas shielding. Especially the last inner cycle generated for layer 1 and 3 reveals that the inner area of the turbine blade can be potentially underfilled, if the molten weld material in the upcoming layers is not streaming into these gaps.

The intermixing in the linkage and the typical grain structure of hot rolled steel can be recognized in the close-ups of the substrate. The 316L metal powder usually forms coarse grains during welding [7]. The grain structure on the borders of both samples (area marked with dotted lines) tend to be orientated in height-direction because the heat continuously flows downward. In the rest of both samples no predominant grain orientation can be distinguished.

After etching the cross sections the austenitic gamma phase turned blue and the delta-ferrite phase became red. Both cross sections show that the austenitic phase is the dominant phase within the built sample, as would be expected from a purely austenitic 1.4404 steel. However, smaller areas of delta-ferrite can be observed in the red circled areas as well. The ferrite area of the direction-parallel sample occurs in the center of the upper layers and center-right in the lower layers. For the contour-parallel sample, the area mostly appeared in the center. Similar observations of the ferrite occurance using the 316L steel as weld material were made by Yadollahi et al. [8], who attribute the ferrite formation to overheating of the materials

In both samples the ferrite-regions tend to be in the center due to the higher heat input. It seems that the direction-parallel sample has a larger ferrite-region in the lower layers compared to the contour-parallel sample. One reason could be that the zigzag-shaped infill paths are causing high heat inputs locally, because the processing head is only slowly moving over the whole surface. On the contrary, the contour-parallel approach created paths, where the laser is quickly moving from one end to the other, thus distributing the heat input over the whole part instead of inducing high amounts of heat locally.

The different planning approaches are visible in the linkage between the manufactured part and the base plate. For the direction-parallel method, the connection line is straight except at the borders. The vaults on both ends indicate the boundary contour which is deposited prior to the zigzag-shaped infill-paths. The linkage between the base plate and the contour-parallel sample (Figure 5c and 5f) consists of continuous vaults showing that the original boundary contour was shrunk continuously in order to fill the area. The areas marked by the green border are indicating the typical layer structure for each strategy as well. For the direction-parallel approach the switching between inclination angles of 45° and 135° is displayed by a flat and a vaulted layer. The different distances between infill cycles of the contour-parallel method are visible as two vaulted layers which are shifted against each other.

Conclusion

In this work, an automated approach to generate zig-zag and contour-parallel infill paths for additive manufacturing LMD was shown. The following conclusions were reached

- An automated zig-zag pattern generation relies on six steps and a coninuous infill is dependent on a monotone outline of a given slice. This can be adjusted by the inclination angle
- Contour-parallel paths are generated by offsetting the contours inwards- or outwards. Two special cases were considered where contours “collide” while generating the path.
- Two turbine-blade shaped paths were built and the cross sections showed a good material quality with elongated, coarse grains common in additive manufacturing
- Porosity in the new material was low and the formation of ferritic phases was attributed to local overheating.

Future work will aim to transfer the generated paths into numerical simulation models to visualize the temperature and optimize the build (e.g. lower overheating).

Acknowledgments

The IGF-project 18737N of the research association Forschungsvereinigung Stahlanwendung e.V. (FOSTA), Sohnstraße 65, 40237 Dusseldorf, was funded through the AiF within the program of the promotion of the industrial joint research (IGF) by the Federal Ministry for Economic Affairs and Energy based on a resolution of the Deutsche Bundestag.

References

[1] B. Graf, S. Ammer, A. Gumenyuk, M. Rethmeier, “Design of Experiments for Laser Metal Deposition in Maintenance, Repair and Overhaul Applications,” *Procedia CIRP*, vol. 11, pp. 245–248, 2013.

[2] A. H. Nickel, D. M. Barnett, F. B. Prinz, “Thermal stresses and deposition patterns in layered manufacturing,” *Materials Science and Engineering: A*, vol. 317, no. 1-2, pp. 59–64, 2001.

[3] E. Foroozmehr and R. Kovacevic, “Effect of path planning on the laser powder deposition process: Thermal and structural evaluation,” *Int J Adv Manuf Technol*, vol. 51, no. 5-8, pp. 659–669, 2010.

[4] M. Biegler, A. Marko, B. Graf, M. Rethmeier, “Finite element analysis of in-situ distortion and

bulging for an arbitrarily curved additive manufacturing directed energy deposition geometry," *Additive Manufacturing*, vol. 24, pp. 264–272, 2018.

[5] E. R. Denlinger, J. C. Heigel, P. Michaleris, T. A. Palmer, "Effect of inter-layer dwell time on distortion and residual stress in additive manufacturing of titanium and nickel alloys," *Journal of Materials Processing Technology*, vol. 215, pp. 123–131, 2015.

[6] OC Oerlikon, *Material Product Data Sheet Austenitic Stainless Steel Powder for Thermal Spray.* [Online] Available: https://www.oerlikon.com/ecomaXL/files/metco/oerlikon_DSMTS-0078.5_AusteniticPowders.pdf&download=1. Accessed on: Aug. 24 2017.

[7] M. Biegler, B. Graf, M. Rethmeier, "In-situ distortions in LMD additive manufacturing walls can be measured with digital image correlation and predicted using numerical simulations," *Additive Manufacturing*, vol. 20, pp. 101–110, 2018.

[8] A. Yadollahi, N. Shamsaei, S. M. Thompson, D. W. Seely, "Effects of process time interval and heat treatment on the mechanical and microstructural properties of direct laser deposited 316L stainless steel," *Materials Science and Engineering: A*, vol. 644, pp. 171–183, 2015.